



Fermi National Accelerator Laboratory

FERMILAB-FN-653

On Crossing Angle at TeV33

V.D. Shiltsev

*Fermi National Accelerator Laboratory
P.O. Box 500, Batavia, Illinois 60510*

February 1997

Disclaimer

This report was prepared as an account of work sponsored by an agency of the United States Government. Neither the United States Government nor any agency thereof, nor any of their employees, makes any warranty, expressed or implied, or assumes any legal liability or responsibility for the accuracy, completeness, or usefulness of any information, apparatus, product, or process disclosed, or represents that its use would not infringe privately owned rights. Reference herein to any specific commercial product, process, or service by trade name, trademark, manufacturer, or otherwise, does not necessarily constitute or imply its endorsement, recommendation, or favoring by the United States Government or any agency thereof. The views and opinions of authors expressed herein do not necessarily state or reflect those of the United States Government or any agency thereof.

Distribution

Approved for public release; further dissemination unlimited.

N.M.

On Crossing Angle at TeV33

V. D. Shiltsev

Fermi National Accelerator Laboratory

P.O.Box 500, Batavia, Illinois 60510

February 7, 1997

Abstract

In this article we study effects of finite crossing angle at collision point on beam dynamics in the Tevatron collider upgrade (TeV33). Impact of the beam-beam interaction on beam sizes, particles diffusion and luminosity is studied with use of computer simulations. Parameter space for better collider performance is proposed. The results are compared with theoretical predictions and experimental data from several hadron and electron machines which exploit the crossing angle.

1 Introduction

The Tevatron collider upgrade (TeV33) [1] intends to operate with some hundred bunches in each beam. Large number of bunches N_b results in small bunch spacing of 132 ns (or about 40 m) and, therefore, collisions occur more frequently. Such a manner to increase the luminosity of the machine where colliding beams share the same vacuum chamber yields in $2(N_b - 1)$ parasitic collisions besides specially designed interaction points (IPs). Detrimental effects of the parasitics collisions of high current beams can be reduced by separation of the orbits of p and \bar{p} beams everywhere except the IPs. However, due to limited space available and limited strength of electrostatic separators several crossing points around the IPs can not be effectively treated in such a way. Collision with crossing angle allows to increase the separation up to a safe value. For design parameters of the TeV33, the half-angle of about $\phi = 0.15\text{--}0.2$ mrad leads to some 2.5–3 rms beam size separation at the first parasitic crossing [2].

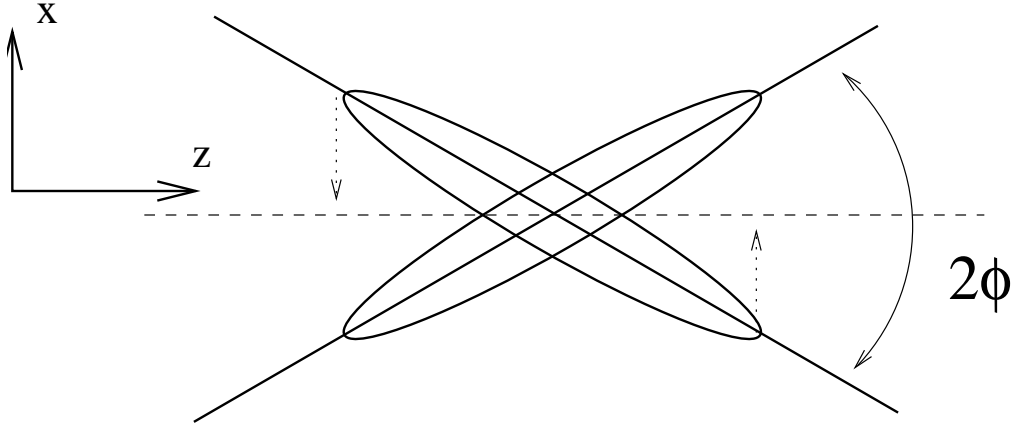


Figure 1: Collision with crossing angle.

There are several consequences of the crossing angle implementation. First of all, collisions with a crossing angle result in geometrical luminosity reduction. Then, in the case of strong electromagnetic interaction between beams, characterized by the beam-beam parameter ξ :

$$\xi = \frac{r_p N_p}{4\pi \varepsilon_n} N_{IP}, \quad (1)$$

(here $r_p = 1.53 \cdot 10^{-18}$ m is the classical proton radius, N_p is the number of particles per bunch, ε_n is the transverse normalized emittance of round beam, and N_{IP} is the number of IPs), the harmful impact of non-linear force due to the opposing beam tends to enhance for particles off the bunch center (at the tail and head). Finally, the coupling between longitudinal and transverse degrees of particle motion causes synchrotron (SB) resonances which are known to limit the performance of several colliders (see Discussion below).

Indeed, if two bunches collide with the crossing angle of 2ϕ , the particles at the head experience an additional transverse kick (toward the other bunch if the bunches have opposite charges) while the particles at the tail get the same kick in opposite direction – see dotted arrows in Fig.1. The total transverse kick $\delta x'$ now depends not only on transverse particles position as in the case of head-on interaction, but also on longitudinal position z within the bunch:

$$\delta x' = f(x + z\phi), \quad (2)$$

here the angle ϕ assumed to be small. The function f describes the beam-beam forces, and in the linear case (for particles with small betatron amplitudes)

$$f(x + z\phi) \approx -(4\pi\xi^{eff}/\beta^*)(x + z\phi),$$

where β^* is the beta-function at the IP, and ξ^{eff} is the *effective* beam-beam parameter [3]:

$$\xi^{eff} = \frac{r_p N_p \beta^*}{2\pi\gamma\sigma_x^{eff}(\sigma_y + \sigma_x^{eff})}, \quad \sigma_x^{eff} = \sqrt{\sigma_x^2 + \sigma_z^2\phi^2}, \quad (3)$$

where $\sigma_{x,y}$ denotes corresponding rms bunch size at the IP, γ is relativistic factor. From. Eq.(3) one can see that a combination of parameters $\Phi = \sigma_z\phi/\sigma_x$ named *normalized or Piwinski angle* plays a role instead of the angle ϕ . In particular, the effective beam-beam parameter for geometrically round beams at IP depends on Φ as

$$\xi^{eff} = \frac{2\xi}{1 + \sqrt{1 + \Phi^2} + \Phi^2}.$$

The longitudinal kick at the IP ΔE also depends on $(x + z\phi)$. As z varies in time performing synchrotron motion, then Eq.(2) reflects a coupling between synchrotron and betatron oscillations¹. Due to non-linearity of the beam-beam forces, numerous synchrotron (SB) resonances can occur at frequencies that in general case satisfy the following relation:

$$n\nu_x + m\nu_y + l\nu_z = \text{integer}. \quad (4)$$

here ν_x, ν_y, ν_z are horizontal, vertical and synchrotron tunes, respectively.

At the moment, nonlinear SB resonances can only be investigated analytically by approximation methods (see cited literature in References) and with use of computer simulations. We employ a recently developed beam-beam simulation code BBC [4]

¹let us note, that, strictly speaking, the SB coupling takes place for head-on collisions without crossing angle too (although the angle strongly enforces the effect). E.g., the change of the particles energy at the collision ΔE is proportional to the product of transverse electric field of the opposing bunch and the particles' trajectory slope at IP $\Delta E \propto \mathcal{E}_x \cdot x'$ – thus, we have an interconnection between the longitudinal and transverse degrees of freedom.

for studies the effects of the crossing angle on beam dynamics in TeV'33. Parameters of the collider, brief description of the code and the simulation results are presented in Section 2. In Section 3 we compare our results with numerical and experimental studies performed for a number of other machines.

2 Simulations with Crossing Angle at TeV33

2.1 Beam-Beam Simulation Code

The BBC code Ver. 3.3 is developed by K.Hirata [4] for the beam-beam simulations in “weak-strong regime” which is close to the TeV33 conditions where proton bunch population is about 6 times the antiproton one. The “weak” (antiproton) bunch was presented by number of test particles, while the “strong” (proton) bunch appeared as an external force of Gaussian bunch. Essential features of the code are:

- a) fully symplectic synchrotron mapping;
- b) Lorentz transformation of the collision with the angle to a head-on collision;
- c) inclusion of the bunch-length effects by using several slices in strong bunch;
- d) variation of the beta function β along the bunch during collision;
- e) energy loss due to longitudinal electric fields are included too.

Typically we tracked 100 (maximum 300) test particles through five slices of strong bunch for $(10-50) \cdot 10^3$ turns. Typical number of 30,000 turns corresponds to about 0.6 s in TeV'33, it is some 100 synchrotron oscillation periods and about the same number of transverse decoherence times due to the beam-beam tune spread [5]. No damping due to radiation or cooling is assumed to play role in the beam dynamics. Further increase of the number of particles as well as number of slices gave almost identical results. Version 3.3 of the BBC code (Dec.1995) assumes the crossing angle only in one plane (e.g. horizontal).

The code outputs of greatest practical utility are luminosity, rms beam sizes and maximum betatron amplitudes which any of the test particles attained during tracking. These outputs are given with respect to unperturbed values, e.g. sizes and amplitudes are divided by their design rms values $\sigma_{x,y}/\sigma_{x,y}^0$ and $A_{x,y}^{max}/\sigma_{x,y}^0$, the luminosity is presented by the reduction factor of $R = L/L_0$ where the bare design luminosity $L_0 = f_0 N_p N_{\bar{p}} / (4\pi \sigma_x \sigma_y)$ and f_0 is the rate of collisions.

2.2 Parameters Set

The relevant parameters of the simulations were chosen close to the TeV33 design ones [1] and presented in the Table 1.

The beam-beam parameter for antiprotons is twice (because of two IPs) the maximum tune shift $\xi = 2 \times N_p r_p / (4\pi \gamma \varepsilon_p)$. We should mention that the presented parameters correspond to injection conditions. They are changing in time, mostly due to intrabeam scattering, and, say, 12 hours after the injection the proton bunch length

Table 1: Set of parameters used in simulations.

Energy	E	1000	GeV
p, \bar{p} /bunch	$(N_p, N_{\bar{p}})$	$(30, 6) \cdot 10^{10}$	
Number of IPs	N_{IP}	1	
Energy spread, rms	$\sigma_E = \Delta E/E$	$2.2 \cdot 10^{-4}$	
Bunch length, rms	σ_z	15	cm
Synchrotron tune	ν_z	0.0045	
Emittance, rms	$\varepsilon_{x,y}$	$3 \cdot 10^{-9}$	m·rad
Beta-function at IP	$\beta_{x,y}^*$	25	cm
\bar{p} Beam-beam parameter	ξ	0.024	
Crossing half-angle (design)	ϕ	$\simeq 0.2$	mrad

is about twice the initial value, antiproton bunch is some 1.7 times longer about 25% less populated, while its transverse emittances is about 50% larger [1].

2.3 Results

First of all, we study the luminosity reduction due to purely geometrical “hour-glass” and beam tilt effects. For that, we used the BBC code with minimum number of turns ~ 10 in order to avoid dynamical effects. From theory [6, 4], it is known that two parameters are important: the bunch length to beta function ratio $S = \sigma_z/\beta^*$ and normalized angle $\Phi = \phi\sigma_z/\sigma^*$. For TeV’33 $S = 0.6$ at the injection and about 1.0 after 12 hours of beam life time; the normalized angle of $\Phi = 1.0$ corresponds to $\phi = 0.183$ mrad. Everywhere below, we remark the set of parameters ξ, Φ, S in our simulations. The simulations of the geometrical luminosity reduction shows the R goes down with either decrease of S or increase of Φ as shown in Figs. 2 and 3 correspondingly. The approximate formulae

$$R \approx \frac{0.96}{\sqrt{1 + \Phi^2}} \quad (5)$$

can be used for the parameter of $S = 0.6$.

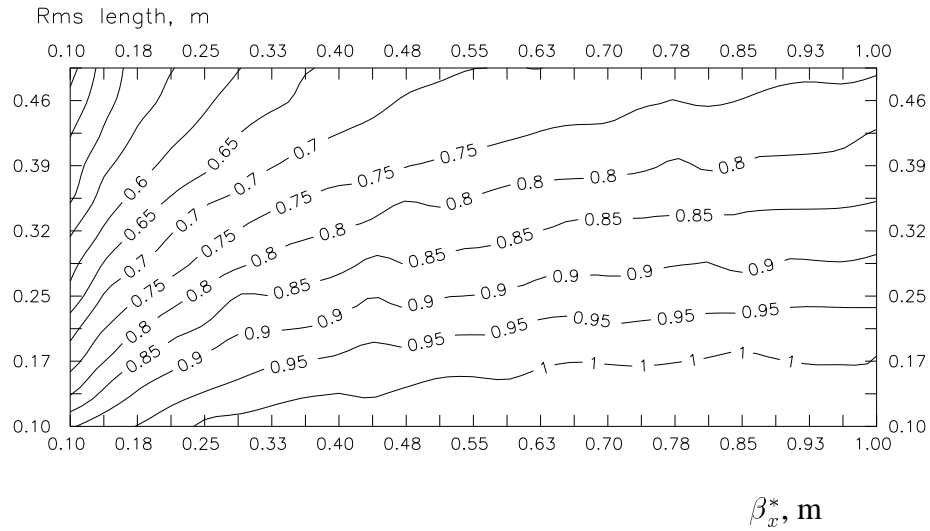


Figure 2: Contour plot of the geometrical luminosity reduction factor R due to “hour-glass” effect vs. bunch length σ_z and beta-function at the IP β^* .

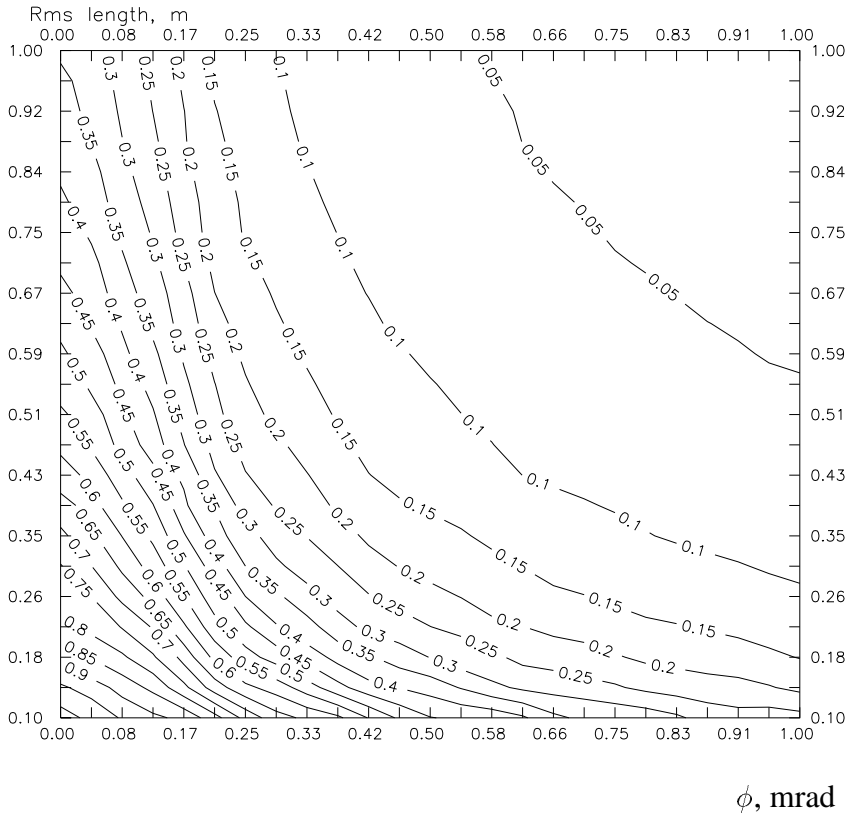


Figure 3: Contour plot of the geometrical luminosity reduction factor R due to tilt effect vs. bunch length σ_z and crossing half-angle ϕ , $\beta^* = 25$ cm.

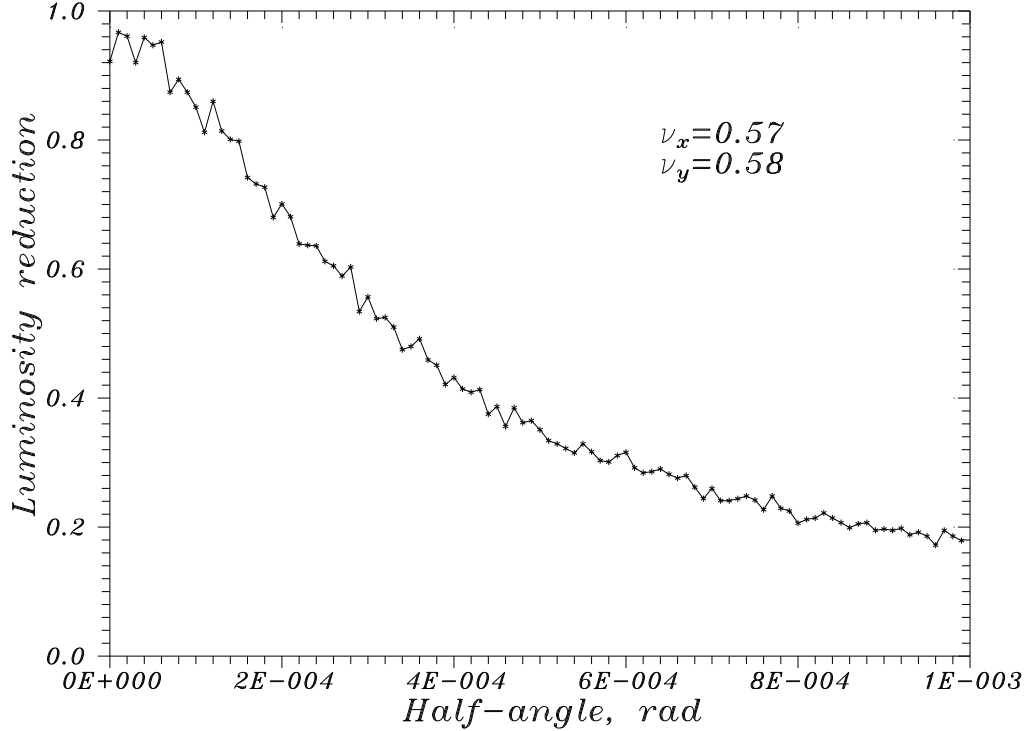


Figure 4: Luminosity reduction factor R vs. crossing angle;
 $\xi = 0.025, \Phi = 0\dots5, S = 0.6.$

One may expect that real reduction of luminosity is affected by dynamical effects due to crossing angle. Nevertheless, at some parameters (the most important among them are the machine tunes and the beam-beam tune shift ξ) the resulting luminosity degradation is about the pure geometrical one as in Eq.(5). Fig.4 shows the factor R vs. ϕ after 30,000 turns under those “good” conditions of $\nu_x = 0.57$, $\nu_y = 0.58$, $\xi = 0.025$. One can see that R is about 0.7 for $\phi = 0.2$ mrad and $R \approx 0.2$ for $\phi = 1$ mrad. At $\phi = 0$ the luminosity factor R is less than 1.0 because of the “hour-glass” effect. No signs of the degradation due to SBRs are seen in Fig.4

Our simulations show that the resonances due to coupling distinctly manifest itself in the growth of the maximum betatron amplitude in the beam. The later is an indicator of transverse particle diffusion which forms a halo and concludes in particles losses. Performing scan over the vertical tune $\nu_y = 0.5\dots1.0$ with $\nu_x = 0.57$, we have found the resonance picture qualitatively changes with increase of the half-angle ϕ . Fig. 5 presents the values of A_x/σ_x^0 (solid curves) and A_y/σ_y^0 (dashed curves) after 10,000 turns vs. ν_y without the crossing angle $\phi = 0$ (upper plot), and with crossing angle of $\phi = 0.2$ mrad (center plot) and $\phi = 0.4$ mrad (bottom plot). First of all, the number resonances grows with ϕ : five of them are seen without the angle, while about ten and twenty at $\phi=0.2$ mrad and 0.4 mrad, respectively, leaving not too much tune space for the collider operation.

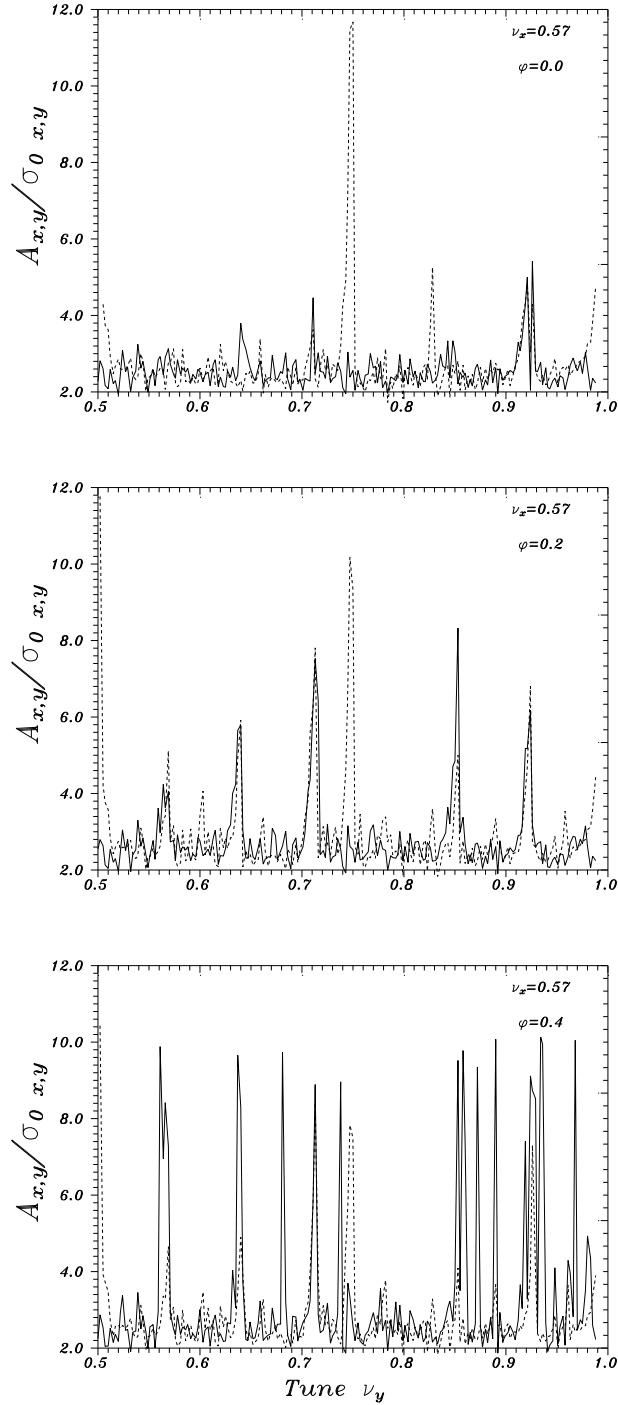


Figure 5: The ν_y dependence of maximum horizontal (A_x - solid) and vertical (A_y - dashed) amplitudes normalized on $\sigma_{x,y}^0$; $\nu_x = 0.57$, $\xi = 0.025$, $S = 0.6$. Crossing angle $\phi = 0$ mrad (upper plot), 0.2 mrad (center plot, $\Phi \simeq 1$), and 0.4 mrad (bottom plot $\Phi \simeq 2$.)

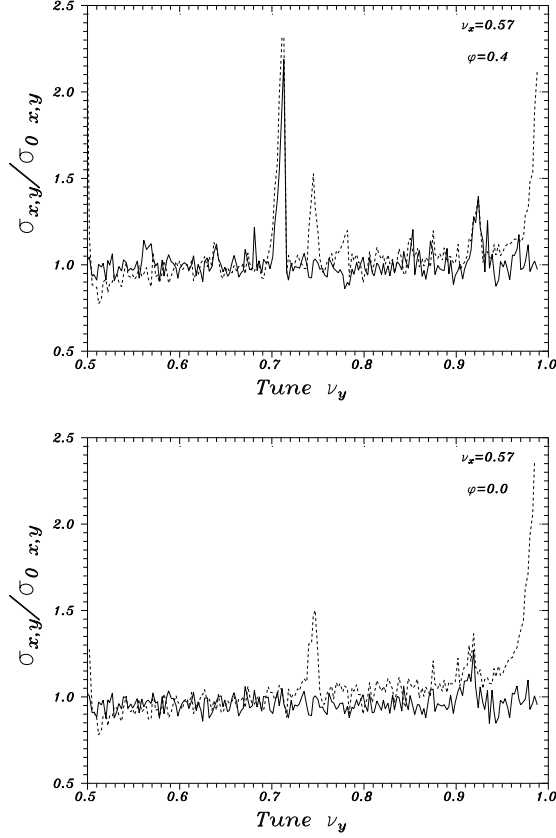


Figure 6: RMS beam sizes $\sigma_{x,y}/\sigma_{x,y}^0$ vs. ν_y , $\nu_x = 0.57$, horizontal-solid line, vertical - dashed; $\xi = 0.025$, $\Phi = 0, 2$; $S = 0.6$

The synchrotron tune is comparatively small - at the particular case presented in Fig.5 $\nu_z = 0.0046$, therefore, the SBRs – at the tunes $\nu_{x,y,z}$ of

$$n\nu_x + m\nu_y + l\nu_z = q,$$

where (n, m, l) and q are integer – look like closely spaced sidebands of (n, m) resonances (line “splitting”).

The major resonances at $\phi = 0$ are $(4,-2)$; $(2,4)$; $(0,4)$; $(0,6)$; $(2,2)$; while a number of new SBRs appears at $\phi = 0.4$ mrad – split line of $(1,-1,\pm 1)$ at $\nu_y = 0.57$, $(4,-2,0)$ and $(4,-2,-2)$ at $\nu_y=0.64$, $(4,4,0)$ at 0.68 , the line of $(2,4)$ resonance becomes wider and larger; the $(0,4,-2)$ sideband of the $3/4$ resonance appears at 0.74 ; then one can see $(2,1,0)$ at 0.86 and $(2,1,2)$ at 0.87 ; split $(2,2)$ lines at 0.93 and $(1,-2,\pm 1)$ at 0.97 ; higher order resonances are seen at $\nu_x = 0.89$ and 0.98 .

One can note, that non-SB resonance at $\nu_y = 0.75$ which is seen even without the angle have smaller maximum amplitudes at larger ϕ , and even its width is slightly shrinking with ϕ . It could be explained by formula (3) which says that effective beam-beam interaction parameter and, therefore, tune spread goes down when the crossing angle Φ grows.

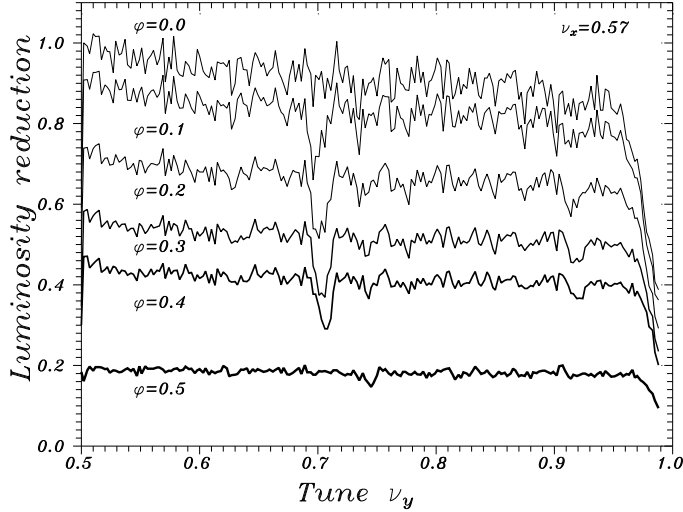


Figure 7: Luminosity reduction factor R vs. vertical tune ν_y ;
 $\nu_x = 0.57$, $\xi = 0.025$, $\Phi = 0, 0.5, 1, 1.5, 2, 2.5$; $S = 0.6$.

The rms beam sizes vs. ν_y without and with 0.4 mrad crossing angle are shown in the bottom and upper plots of Fig.6. The degradation is seen but not as drastic as for the maximum amplitudes in Fig.5. The resulting luminosity reduction is presented in Fig.7, one can conclude that the luminosity is the least sensitive output with respect to the SBR – only drop at $\nu_y = 0.71$ is valuable.

Finally, from Figs. 5,6, and 7 one can conclude that at $\xi = 0.0265$, $\nu_x = 0.57$, there are “windows” in ν_y without SB resonances at 0.51–0.56, 0.58–0.62 and 0.77–0.83. The first two are preferable from the point of larger luminosity. One can expect no resonances there and no enhanced particle losses.

There is a qualitative difference in beam dynamics when the tunes are far from resonances (in the “good windows”) and close to one of the SBRs. Fig.8 demonstrates dependencies of maximum amplitudes on the crossing angle for $\nu_x = 0.57$, $\nu_y = 0.58$ (top plot, off-resonance) and for $\nu_x = 0.58$, $\nu_y = 0.71$ (lower plot). The “off-resonant” case shows no meaningful (over statistical fluctuations) changes in particles diffusion rates with increase of the angle, while at the “bad” operation point the amplitude does not grow until normalized angle of $\Phi \simeq 1$ ($\phi \simeq 0.2$ mrad), then rapidly increases (note the scale difference in upper and lower plots) and slowly decreases. That weakening of the SBR at $\Phi \sim 3 - 5$ is probably due to the fact that the effective beam-beam forces become many times smaller due to the tilt effect. Thus, one may expect larger beam losses rates due to beam-beam interaction if the machine is not tuned properly and the normalized crossing angle is about $\Phi \sim 1 - 2$.

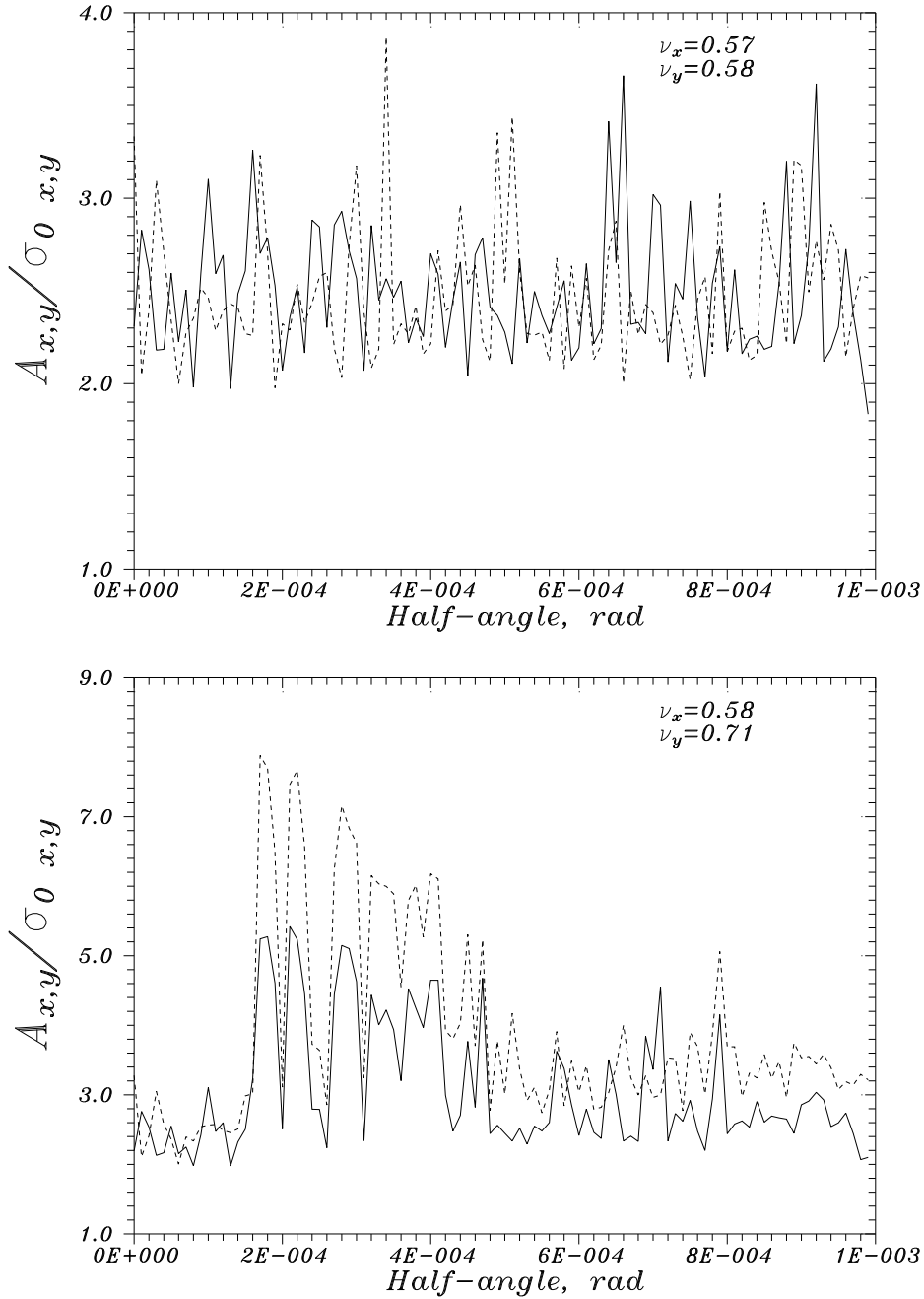


Figure 8: The ϕ dependence of maximum horizontal (A_x - solid) and vertical (A_y - dashed) amplitudes normalized on $\sigma_{x,y}^0$;
upper plot $\nu_x = 0.57$, $\nu_y = 0.58$, $\xi = 0.025$, $\Phi = 0\dots5$, $S = 0.6$;
lower plot $\nu_x = 0.58$, $\nu_y = 0.71$, $\xi = 0.025$, $\Phi = 0\dots5$, $S = 1$.

In order to determine the tune space for better performance we made a 2-D scan over the tune space of ν_x, ν_y (0.55...0.65, 0.55...0.65). Without the crossing angle, the maximum betatron amplitude has no peculiarities as it is shown in Fig.9. The resonance “hills” are clearly seen in the plots of maximum amplitudes of horizontal

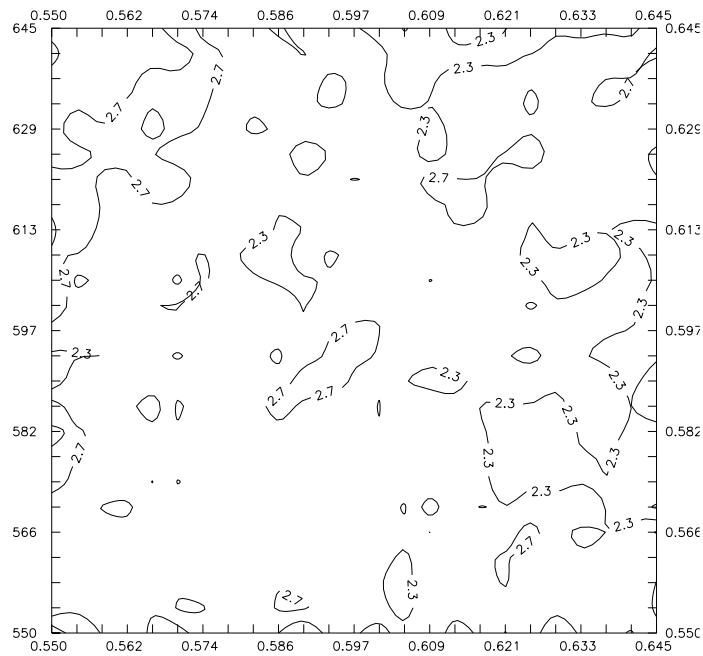
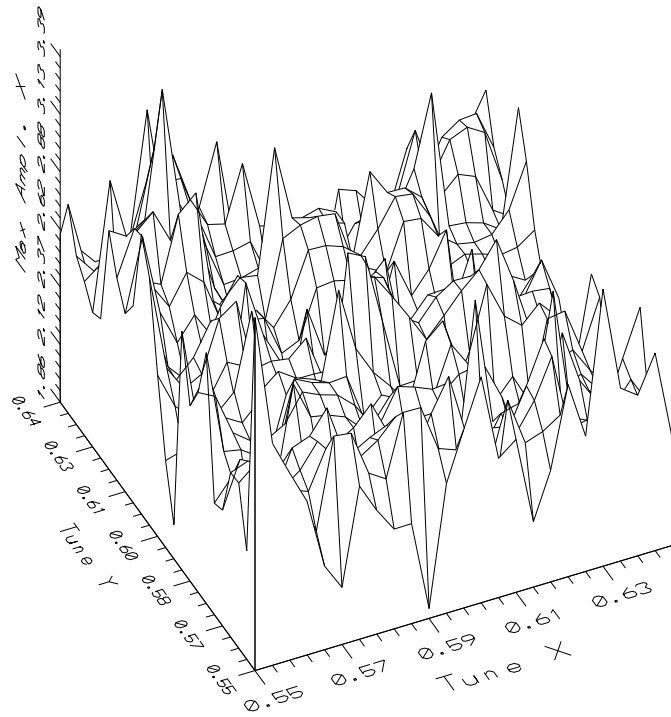


Figure 9: The A_x scan without crossing angle: 3-D (up) and contour plot (down). The abscissa and ordinate are horizontal and vertical tunes, respectively; $\xi = 0.025$, $\Phi = 0$, $S = 0.6$.

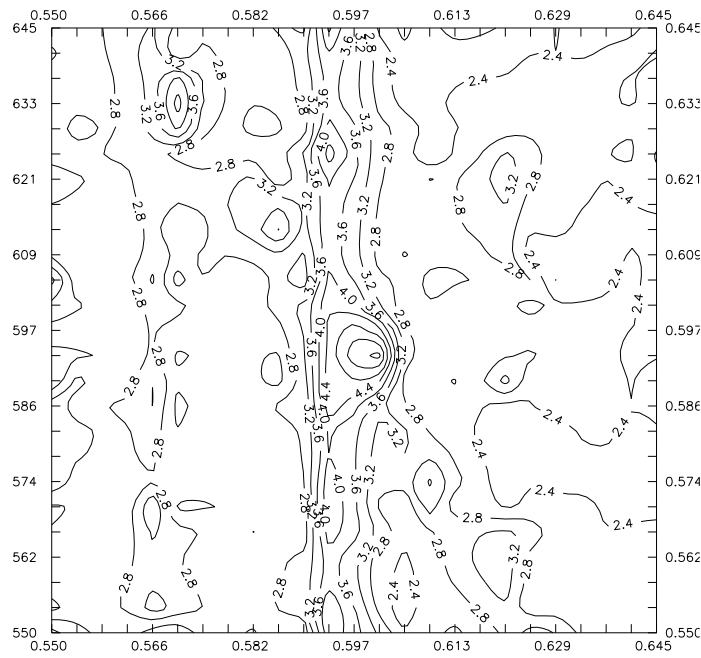
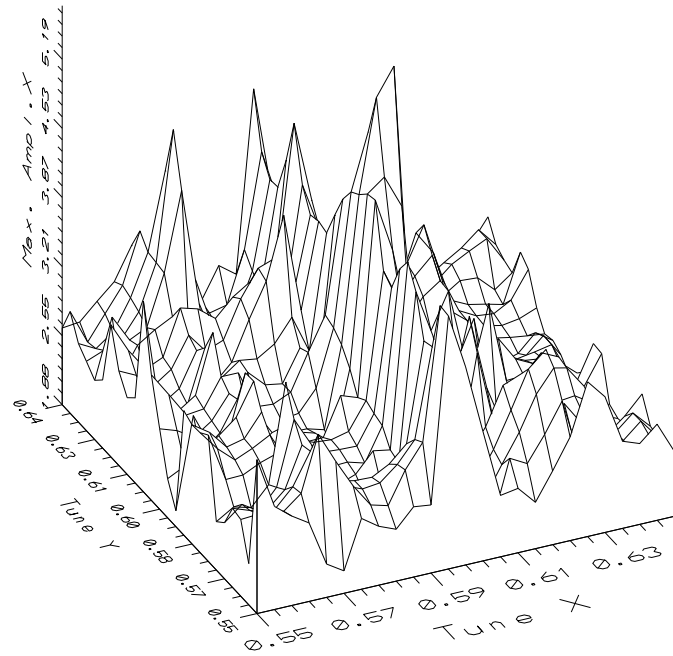


Figure 10: The A_x scan : 3-D (up) and contour plot (down). The abscissa and ordinate are horizontal and vertical tunes, respectively; $\xi = 0.025$, $\Phi = 1$, $S = 0.6$

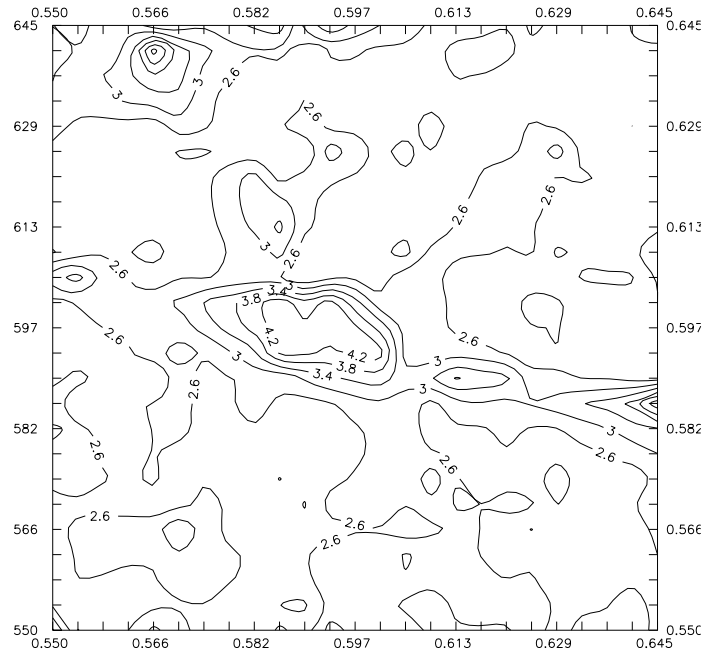
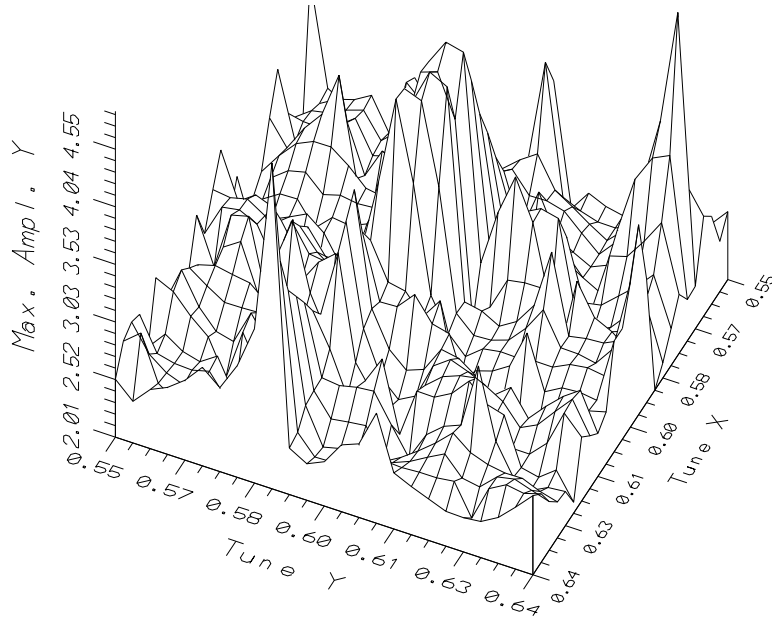


Figure 11: The A_y scan : 3-D (up) and contour plot (down). The abscissa and ordinate are horizontal and vertical tunes, respectively; $\xi = 0.025$, $\Phi = 1$, $S = 0.6$.

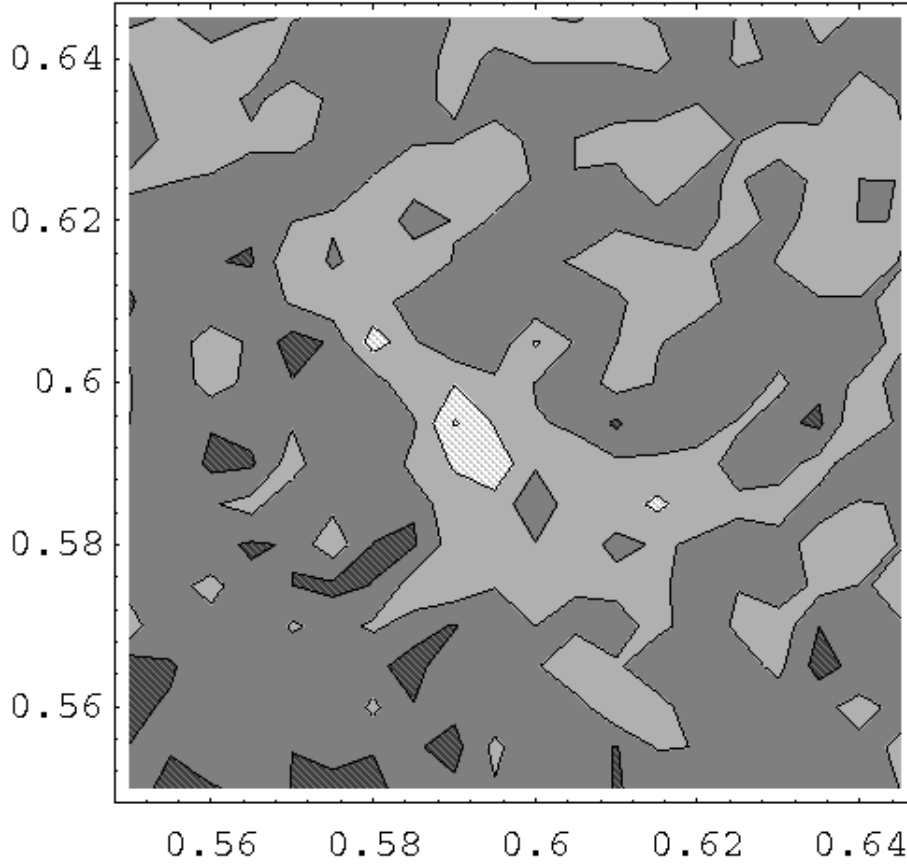


Figure 12: Luminosity contour plot (scan). The abscissa and ordinate are horizontal and vertical tunes, respectively; $\xi = 0.025$, $\Phi = 1$, $S = 0.6$.

and vertical betatron oscillations – see Figs.10 and 11, respectively – if the crossing angle is equal to 0.2 mrad. After only 10,000 turns the ratio of $A_{x,y}/\sigma_{x,y}^0$ could reach values of the order of 5 at some resonance lines, while without the angle they do not exceed 2.7. One can recognize the most valuable resonances in the tune space – they are at $\nu_x \approx 0.59$ and $2\nu_x + \nu_y$ in horizontal dynamics (Fig.10), and at $\nu_x + 3\nu_y$ and $\nu_x + \nu_y$ in the vertical one (Fig.11). Note, that if both tunes are in the area of 0.55–0.59 then the amplitudes are pretty the same for the case of $\phi = 0.2$ mrad and for zero crossing angle.

Fig.12 presents the luminosity reduction factor R contour plot in (ν_x, ν_y) plane. The darker areas correspond to the higher luminosities with maximum R of about 0.9. The contour spacing is 5% in luminosity reduction. One can see, that there several areas with small luminosity where the R is about 0.7. The lower left corner of the plot $0.55 < \nu_x < 0.59$, $0.55 < \nu_y < 0.59$ is rather dark, that means better luminosity conditions.

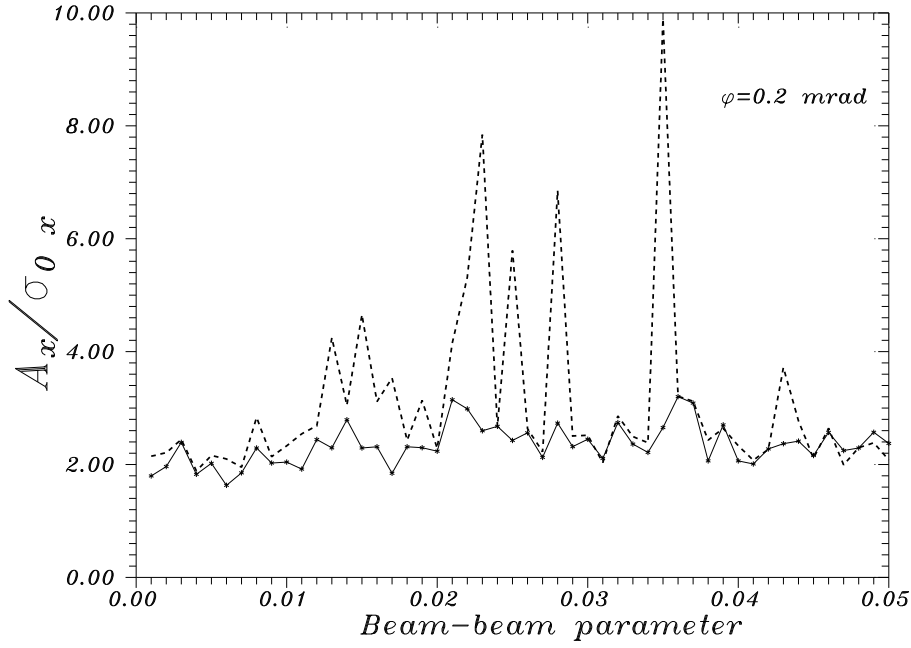


Figure 13: The ξ dependence of maximum horizontal amplitude A_x for $(\nu_x, \nu_y) = (0.57, 0.58)$ - solid line, and $(0.58, 0.71)$ - dashed line; $\Phi = 1$, $S = 0.6$.

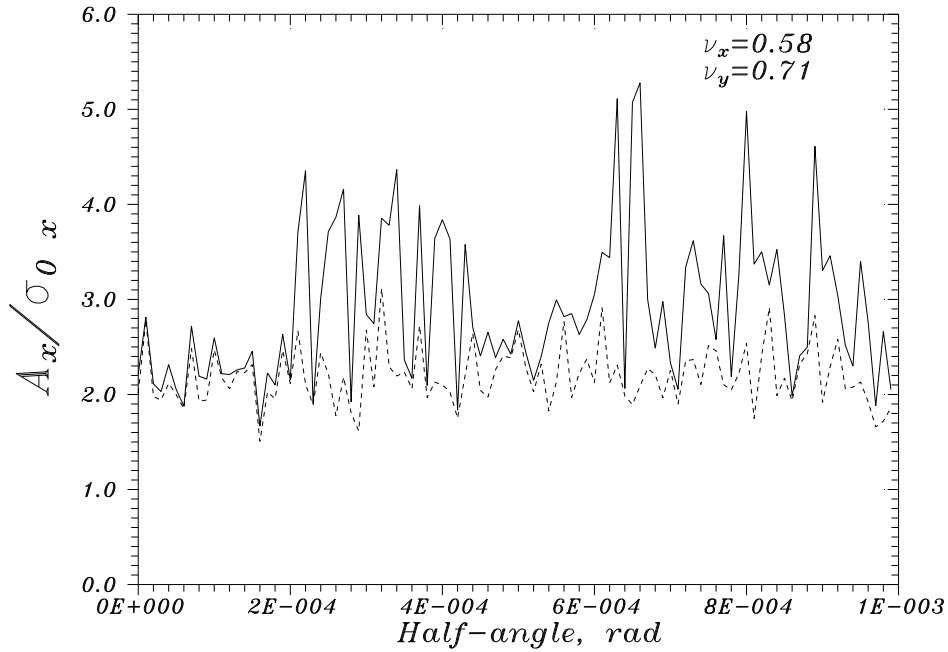


Figure 14: The ϕ dependence of maximum horizontal amplitude A_x/σ_x^0 for $\xi = 0.025$ (solid line), and $\xi = 0.0025$ (dashed line) near resonant working point of $\nu_{x,y} = (0.58, 0.71)$; $S = 0.6$.

Obviously the beam dynamics in the collider depends on the beam-beam parameter ξ (see definition in Eq.(1)). Fig.13 presents the maximum horizontal am-

plitude vs. ξ for the two working points considered above – (0.57,0.58) and (0.58, 0.71). One can see slight and monotonic growth of A_x at the off-resonance point (solid line), while valuable growth is seen at the near-resonant point of (0.58,0.71) if $\xi > 0.01$. Below 0.01 both cases are almost identical.

Simulations with two values of $\xi = 0.025$ and $\xi = 0.0025$ allows to study the impact of the crossing angle on the maximum amplitude nearby the resonance of (0.58,0.71) – results are shown in Figs.13 (solid line is for $\xi = 0.025$, dashed line – for $\xi = 0.0025$). We can see again larger amplitudes at larger ξ and at Φ larger than 1. The Φ dependence above 1 looks rather step-like then growing function.

The question of how stable are “good” working point with respect to numerous machines’ errors, disturbances and distortions has to studied carefully in the future. Among the most realistic imperfections are the beams separation at the interaction points, the tune ripple, coupling and non-linear magnetic field components at the rest of the lattice.

3 Discussion

The model we used in our simulations is not quite adequate to the TeV33 design: first of all, the only interaction point (IP) is taken into account while there are two IPs in the Tevatron collider. It is known that the tunes difference between IPs breaks the symmetry of the collider and can possibly deteriorate the collider performance. The effect is found to be not very detrimental in beam-beam studies for DAΦNE $e^+ - e^-$ collider [7] with use of another version of the BBC code, it is found that it cause only slight reduction in luminosity, so one may dare to consider one IP results as rather precise, although, the two IP simulations would be useful.

Secondly, there is no simulation done for the crossing in two planes as it is supposed in the current TeV33 [1, 2]. However, we note, that in the case of almost equal beam sizes of p and \bar{p} beams at the IP and only slightly different vertical and horizontal tunes the single plane angle model does not seem to be too unrealistic, as long as we do not consider near-crossings interactions.

Some other comments deal with the weak-strong model which is not fully adequate to the Tevatron conditions, then, we take into account no $x - y$ coupling in the rest of the lattice, and finally we track beam over comparatively small number of turns $N_{turns} \leq 30,000$ because of CPU time limitations. Simple check has shown that far off resonances, the calculated luminosity and beam sizes almost don’t depend on N_{turns} , while the maximum betatron amplitudes slightly grow with N_{turns} .

Finally, we conclude that the model used in simulations can not be rejected as unrealistic, although further studies of the issue are necessary.

The major results of this work are:

1. out of resonances only geometrical luminosity degradation R_G is expected for the TeV33 with non-zero crossing angle ϕ in the range of 0...1 mrad. The approximation formulae for the reduction is $R_G = L_G/L_0 \simeq 0.95/\sqrt{1 + \Phi^2}$,

where $\Phi = \phi\sigma_z/\sigma_x$ is “normalized” (horizontal) angle, and factor of 0.95 is due to hour glass effects at $S = \sigma_z/\beta^* \approx 0.6$.

2. over the tune space of $0.55 < \nu_x, \nu_y < 0.59$ we observe almost no enhanced particle losses with crossing angle less than 0.2 mrad $\Phi < 1$.
3. other tune areas are influenced by synchrobetatron resonances, and dangerous increase of the loss rate occurs at $\Phi \gtrsim 1$ ($\phi \gtrsim 0.2$ mrad). The beam size or maximum betatron amplitudes do not grow monotonically with increase of Φ – instead, they are rather be constant or even decrease slightly.
4. simulations result in large maximum betatron oscillation amplitudes in both horizontal and vertical planes at and nearby specified resonances, that means enforced losses of particles.
5. the effects are found to be larger for larger beam-beam parameter ξ .
6. the effects of tune ripple, coupling and sextupole fields in the rest of the lattice, two IPs instead of one, smaller synchrotron tune, beam separation at the IPs, and the crossings angle in two planes need further studies. The BBC code can also be used for investigation of the parasitic crossings effect.

Let us compare our results with studies made at (or for) other colliders with non-zero crossing angle at interaction points. Because of qualitative differences in beam dynamics we present results for electron-positron and hadron colliders separately in Tables 2 and 3.

Historically, electron storage rings had implemented multibunch regime of operations in late 70’s – early 80’s and the crossing angle was checked as a solution for elimination parasitic collisions. Since that time a number of colliders got an experience with the crossing angle. Initially, it was observed at DORIS I [8] that as many as 24 additional vertical SB resonances (all other machines in Table 2 had the angle in horizontal plane) which made impossible high luminosity operation of the collider. The normalized angle Φ was of the order of 0.5. As electron storage rings have comparably large synchrotron tunes, the synchrobetatron resonances cover the tune space in rather dense way, leaving pretty tiny “safe” tune areas. After DORIS, all the colliders use the normalized angles smaller than 0.2 and mostly in horizontal plane (in electron machines the horizontal size is typically many times larger than vertical one, that allows larger geometrical angle ϕ for the same value of Φ). Experiments at CESR [9], LEP [10] and simulations for Frascati ϕ -factory DAΦNE [7] show that under these conditions the luminosity degradation due to SBR can be acceptable or even negligible.

The hadron colliders stand out by absence of the cooling due to synchrotron radiation, much smaller values of synchrotron tune, and smaller beam-beam parameter

Table 2: Electron-Positron Colliders

	DAΦNE [7]	CESR [9]	DORIS [8]	LEP [10]
Energy, GeV	0.51	5	3.5-5	45
Bunches/beam	1	3(7,9)	120	4×4
Bunch length σ_z , cm	3	1.8	2.4	1.5
IP bunch size σ_x , μm	2200	550	580	7.5 (v)
Half-angle ϕ_x , mrad	12.5	2.5	12	0.03
Norm. angle, $\phi_x\sigma_z/\sigma_x$	0.18	0.1	0.45	0.1
Beam-beam shift, ξ_x	0.04	0.04	0.03	~ 0.02
Synchr. tune $\nu_z \times 10^2$	1.2	8	3	~6
Comments	simul. high L	exper. high L	exper. lots SBR	exper. high L

ξ with respect to the electron rings. Without the damping, dynamical particle diffusion due to SB resonances could be much more dangerous than for electrons, but due to smaller ξ the synchrotron coupling itself is weaker, moreover, smaller ν_z leaves larger tune areas for “safe” operation. The only experimental result shown in Table 3 was obtained at the SPS(CERN) collider in 1985 [11]. There was found no SB luminosity reduction and no substantial particle loss increase with parameters of $\Phi = 0.5$, $\xi=0.02$ and $\nu_z = 0.005$. We should emphasize that the TeV’33 parameters are close to the SPS experiment ones (except twice larger Φ), therefore, our “optimistic” conclusions about SB dynamics are somehow consistent with the previous experience. Simulations for HERA $e - p$ collider (see A.Piwinski in [12]) have shown that initial design value of 10 mrad crossing angle, i.e. $\Phi = 5$, leads to substantial luminosity reduction, and as the result, the angle was eliminated at all. Recent numerical studies of T.Sen [12] result in acceptability of 2 mrad angle, Φ about 1². The LHC design [13] intends to collide the beams with $\Phi \simeq 0.5$ without beam degradation.

Acknowledgments

²in series of works [6, 8, 12, 14], a simplified model of beam-beam interaction is used which consider the beam-beam kick taking place at one point, i.e. the opposite beam is presented as a single slice which produces approximate *effective* force. Later it was pointed in [15] that such an approach somewhat overestimate the strength of SB resonances. The BBC code takes all these and other known effects into account.

Table 3: Proton Colliders (pp , $p\bar{p}$, pe)

	SPS [11]	HERA [12]	TeV33	LHC [13]
Proton energy, GeV	400	820	1000	7000
Bunches/beam	3	210	108	2835
Bunch length σ_z , cm	50	13	14	7.5
IP bunch size σ_r , μm	163	230	35	16
Half-angle ϕ , mrad	0.175	10 (2)	0.2	0.1
Norm. angle, $\Phi = \phi\sigma_z/\sigma_r$	0.5	5(~ 1)	~ 1	0.5
Beam-beam shift, $\xi \times 10^2$	$\simeq 2$	0.04	2.4	0.34
Synchr. tune $\nu_z \times 10^2$	0.5	0.08	0.46	0.2
Comments	exper. high L	simul. $\phi = 10$ - very bad $\phi = 2$ - accept.	simul. accept.	simul. high L

Author thanks K. Hirata(KEK) for an opportunity to use his simulation code and his helpful advises concerning its operation. Valuable comments and fruitful discussions with M. Zobov(Frascatti), A. Piwinski (DESY), V.Danilov (Budker INP), P. Bagley, J. Marriner, D. Finley and L. Michelotti (FNAL) are sincerely acknowledged. I am thankful to N. Gelfand and O. Krivosheev for their help with the BBC code compilation and launching.

References

- [1] J.P.Marriner, “The Fermilab Proton-Antiproton Collider Upgrades”, FERMILAB-Conf-96/391 (1996);
S.D.Holmes, *et.al*, FNAL-TM-1920 (1995).
- [2] P.P.Bagley, *et.al.*, “Summary of the TeV33 Working Group”, FERMILAB-Conf-96/392 (1996).
- [3] A.Piwinski, *Proc. III Advanced ICFA Beam Dynamics Workshop* (Novosibirsk, 1989), p.12.
- [4] K.Hirata, *Phys. Rev. Lett.*, 74, p.2228 (1995).;
K.Hirata, SLAC-Pub-6375 (1994);

- K.Hirata, KEK Preprint 93-190 , KEK (1993);
 K.Hirata, H.Moshhammer, F.Ruggiero, *Particle Accelerators*, 40, p.205 (1993).
- [5] G.Stupakov, V.Parkhomchuk, V.Shiltsev, SSCL-Preprint-495 (1993).
- [6] A.Piwinski, DESY Report 77-18 (1977).
- [7] K.Hirata, M.Zobov, “Beam-Beam Interaction Studies for DAFNE”, *Proc. 1996 EPAC*, Barcelona, Spain (1996), p.1158.
- [8] A.Piwinski, IEEE Trans., NS-24, No.3 (1977), p.1408.
- [9] A.V.Temnykh, et.al, *1993 IEEE PAC*, Washington DC (1993), p.2007;p.3476;
 D.Rice, *ibid.*, p.1978;
 A.V.Temnykh, CBN 93-1 (Cornell Univ., 1993);
 D.L.Rubin, et.al, NIM A330 (1993), p.12.
- [10] O.Brunner, et.al, *Proc. of 1995 IEEE PAC*, Dallas (1995), p.514;
- [11] L.R.Evans, A.Faugier, R.Schmidt, IEEE Trans., NS-32, No.5 (1985), p.2209.
- [12] A.Piwinski, IEEE Trans., NS-26, No.3 (1979), p.3604;
 A.Piwinski, IEEE Trans., NS-32, No.5 (1985), p.2240;
 A.Piwinski, AIP Conf. Proc., 326, (1995), p.202;
 T.Sen, DESY HERA 96-02 (1996).
- [13] LHC Conceptual Design, CERN-AC-95-05 (LHC) (1995).
- [14] A.Piwinski, SSC-57 (1986);
 A.Piwinski, AIP Conf. Proc., 326, (1995), p.202.
- [15] S.Krishnogopal, R.Siemann, *Phys. Rev. D*, v.41 (1990), p.2312.